

MARVEL Analysis of the Measured High-Resolution Rovibronic Spectra and Definitive Ideal-Gas Thermochemistry of the $^{16}\text{O}_2$ Molecule

Cite as: J. Phys. Chem. Ref. Data **48**, 023101 (2019); <https://doi.org/10.1063/1.5083135>

Submitted: 28 November 2018 . Accepted: 06 March 2019 . Published Online: 10 April 2019

Tibor Furtenbacher , Mátyás Horváth, Dávid Koller, Panna Sólyom, Anna Balogh, István Balogh, and Attila G. Császár 

COLLECTIONS

 This paper was selected as Featured



[View Online](#)



[Export Citation](#)



[CrossMark](#)

ARTICLES YOU MAY BE INTERESTED IN

Improved high-resolution spectroscopic data for molecular oxygen
Scilight **2019**, 150006 (2019); <https://doi.org/10.1063/1.5097544>

Definitive Ideal-Gas Thermochemical Functions of the H_2^{16}O Molecule
Journal of Physical and Chemical Reference Data **45**, 043104 (2016); <https://doi.org/10.1063/1.4967723>



Where in the **world** is AIP Publishing?
Find out where we are exhibiting next



MARVEL Analysis of the Measured High-Resolution Rovibronic Spectra and Definitive Ideal-Gas Thermochemistry of the $^{16}\text{O}_2$ Molecule

Cite as: J. Phys. Chem. Ref. Data 48, 023101 (2019); doi: 10.1063/1.5083135

Submitted: 28 November 2018 • Accepted: 6 March 2019 •

Published Online: 10 April 2019



View Online



Export Citation



CrossMark

Tibor Furtenbacher,¹  Mátyás Horváth,² Dávid Koller,² Panna Sólyom,³ Anna Balogh,³ István Balogh,³ and Attila G. Császár^{4,a)} 

AFFILIATIONS

¹ MTA-ELTE Complex Chemical Systems Research Group, Pázmány Péter sétány 1/A, H-1117 Budapest, Hungary

² Eötvös József Gimnázium, Reáltanoda utca 7, H-1053 Budapest, Hungary

³ Tatai Református Gimnázium, Kossuth tér 11, H-2890 Tata, Hungary

⁴ Laboratory of Molecular Structure and Dynamics, Institute of Chemistry, ELTE Eötvös Loránd University and MTA-ELTE Complex Chemical Systems Research Group, Pázmány Péter sétány 1/A, H-1117 Budapest, Hungary

^{a)} Author to whom correspondence should be addressed: csasarag@caesar.elte.hu

ABSTRACT

Accurate, empirical rovibronic energy levels, with associated uncertainties, are determined for the lowest seven electronic states of the $^{16}\text{O}_2$ molecule using the MARVEL (Measured Active Rotational-Vibrational Energy Levels) algorithm. After careful analysis and validation of 30 671 rovibronic transitions (including 24 376 measured and 6295 artificial transitions), collected from 91 publications, 4279 empirical rovibronic energy levels are determined. The highly accurate empirical (MARVEL) energy database is then augmented with rovibronic energies obtained from accurate effective Hamiltonians for the lowest six electronic states, establishing a hybrid database containing 15 946 rovibronic energy levels. Based on this hybrid database, complete up to the first dissociation limit, $41\,260\text{ cm}^{-1}$, an accurate temperature-dependent ideal-gas partition function, $Q_{\text{int}}(T)$, and some related thermochemical functions [isobaric heat capacity, $C_p^{\circ}(T)$, entropy, $S^{\circ}(T)$, and (absolute) enthalpy, $H^{\circ}(T)$] are derived for $^{16}\text{O}_2$ employing the direct-summation technique. All thermochemical functions are reported, in 1 K increments up to 5000 K, in the supplementary material to this paper.

Published by AIP Publishing on behalf of the National Institute of Standards and Technology. <https://doi.org/10.1063/1.5083135>

Key words: high-resolution spectroscopy; ideal-gas thermochemistry; O_2 ; oxygen; partition functions; rovibronic energy levels.

CONTENTS

1. Introduction	2
2. Methodological Details	3
2.1. MARVEL	3
2.2. Quantum numbers	3
2.3. Electronic states of the $^{16}\text{O}_2$ molecule	3
3. Overview of the Literature	3
4. MARVEL Energy Levels	4
5. The Hybrid Dataset	7
6. Ideal-Gas Partition and Thermochemical Functions	8
7. Summary and Conclusions	11
8. Supplementary Material	11
Acknowledgments	11
9. References	11

List of Tables

1. Electronic states of O_2 present in the MARVEL database collated during the present study, their notation, and the characterization of the experimental spectroscopic information available for them	4
2. Characterization of the experimental rovibronic transitions present in the MARVEL database	4
3. Characteristics of data sources related to the $^{16}\text{O}_2$ molecule and analyzed during the present study, where A and V stand for the available and validated entries in a given source, respectively	5
4. Number of energy levels and the average rotational quantum number (J) in different energy regions	8

5. Temperature-dependent ideal-gas internal partition function with estimated uncertainties in parentheses (in units of the last quoted decimal place), $Q_{\text{int}}(T)$, of the $^{16}\text{O}_2$ molecule at selected temperatures obtained by different sources
 9
6. Ideal-gas enthalpy with estimated uncertainties in parentheses (in units of the last quoted decimal place), $H^0(T)$ (in J mol^{-1}), of the $^{16}\text{O}_2$ molecule at selected temperatures T obtained by different sources
 10
7. Ideal-gas isobaric heat capacity with estimated uncertainties in parentheses (in units of the last quoted decimal place), $C_p^0(T)$ (in $\text{J mol}^{-1} \text{K}^{-1}$), of the $^{16}\text{O}_2$ molecule at selected temperatures T obtained by different sources
 10

List of Figures

1. Experimentally characterized band system of the $^{16}\text{O}_2$ molecule
 2
2. Differences between the empirical (MARVEL) energy levels of this study and the earlier literature results of 86Ramsay, 99JeMeCoCa, and 99YoEsPaTh, all related to the $c\ ^1\Sigma_u^-$ electronic state of $^{16}\text{O}_2$
 6

3. Differences between the empirical (MARVEL) energy levels and the earlier literature results of 86BoBoRa, 94YoMuEsSu, and 99JeMeCoCa, all related to the $A\ ^3\Sigma_u^+$ electronic state of $^{16}\text{O}_2$
 6
4. Differences between the empirical (MARVEL) energy levels and the earlier results of 86CoRa and 99JeMeCoCa on the $A'\ ^3\Delta_u (\Omega = 1)$ state of $^{16}\text{O}_2$
 6
5. Differences between the empirical (MARVEL) energy levels and the earlier results of 86CoRa and 99JeMeCoCa on the $A'\ ^3\Delta_u (\Omega = 2)$ state of $^{16}\text{O}_2$
 6
6. Differences between the empirical (MARVEL) energy levels and the earlier results of 86CoRa and 99JeMeCoCa on the $A'\ ^3\Delta_u (\Omega = 3)$ state of $^{16}\text{O}_2$
 7
7. Differences between the empirical (MARVEL) energy levels and the earlier literature results of 05HaDuUb, 03MaChLeYo, 96ChYoEsPa, and 86ChYoPaFr related to the $B\ ^3\Sigma_u^-$ electronic state
 7
8. The contribution of Q^{missing} (solid line) and Q''^{missing} (dashed line) in % at different temperatures
 8
9. Uncertainty of the partition function (solid line) and its second moment (dashed line) using the “two extrema” method
 9

1. Introduction

Dioxygen, O_2 , is the second most abundant molecule in the Earth’s atmosphere. O_2 , due to the open-shell nature of its ground electronic state as well as the existence of several low-lying excited electronic states (see Fig. 1), is characterized by highly complex rovibronic spectra, extending from the microwave (MW) to the ultraviolet (UV). Over the last 100 years, the desire to understand the spectroscopy of dioxygen^{1–99} has led to a number of fundamental advances in chemistry and molecular physics.

Since O_2 is one of the most important chemical and “biochemical” molecules, several comprehensive reviews^{15,22,46,89,92–94,100,101} have been published on its spectroscopy and quantum dynamics. Probably the first modern review on O_2 spectroscopy was written in 1962, when Wallace¹⁵ collected the vibrational band centers for several important molecules, including dioxygen. In 1972, Krupenie²² collected all measured and calculated (predicted) data for O_2 , as well as of the related ions O_2^+ , O_2^- , and O_2^{2-} . In their justly famous book, Huber and Herzberg¹⁰⁰ collected the most important spectroscopic

constants of several electronic states of $^{16}\text{O}_2$, $^{16}\text{O}_2^+$, $^{16}\text{O}_2^{2+}$, and $^{16}\text{O}_2^-$. In 1988, Slanger and Cosby⁴⁶ published new and improved spectroscopic constants for the six lowest electronic states of $^{16}\text{O}_2$ (see Fig. 1). During the last decade, the Jet Propulsion Laboratory (JPL)^{89,92–94} published a series of articles on O_2 spectroscopy, which have been accompanied by spectroscopic databases. In the JPL compilations of experimental measurements on O_2 , the authors critically compiled the measured transitions of six isotopologues: $^{16}\text{O}_2$, $^{17}\text{O}_2$, $^{18}\text{O}_2$, $^{16}\text{O}^{17}\text{O}$, $^{16}\text{O}^{18}\text{O}$, and $^{17}\text{O}^{18}\text{O}$. The aim of the JPL project has been the examination and simultaneous fit of the MW, terahertz (THz), infrared (IR), visible, and UV rovibronic data of the six dioxygen isotopologues mentioned using a global Dunham model and prediction of all the measured and as yet unmeasured transitions for the lowest three electronic states ($X\ ^3\Sigma_g^-$, $a\ ^1\Delta_g$ and $b\ ^1\Sigma_g^+$, see Fig. 1). The JPL studies also collected a lot of measured transitions for the Schumann–Runge system ($B\ ^3\Sigma_u^-$ – $X\ ^3\Sigma_g^-$), the Chamberlain system ($A'\ ^3\Delta_u$ – $a\ ^1\Delta_g$), and the Herzberg III system ($A'\ ^3\Delta_u$ – $X\ ^3\Sigma_g^-$) (see Fig. 1).

Since the availability of accurate electronic potential energy surfaces helps to understand the structure and the dynamic behavior of molecules and to interpret even complex observed high-resolution spectra, a considerable number of articles addressed the potential energy curves (PECs) of molecular oxygen, depending just on the OO distance. Without attempting to be comprehensive, here are a few important publications about the computation of O_2 PECs: Vanderslice *et al.*,¹⁰² Schaefer and Harris,¹⁰³ Beebe *et al.*,¹⁰⁴ Saxon and Liu,¹⁰⁵ and Liu *et al.*¹⁰⁶

O_2 is molecule number 7 in the canonical spectroscopic database HITRAN (High-Resolution Transmission Molecular Absorption). In the most recent HITRAN2016 edition,¹⁰⁷ there are 1897 rovibronic transitions reported for O_2 , involving three electronic states ($X\ ^3\Sigma_g^-$, $a\ ^1\Delta_g$, and $b\ ^1\Sigma_g^+$) and the atmospheric, the IR atmospheric, and the Noxon band systems (Fig. 1).

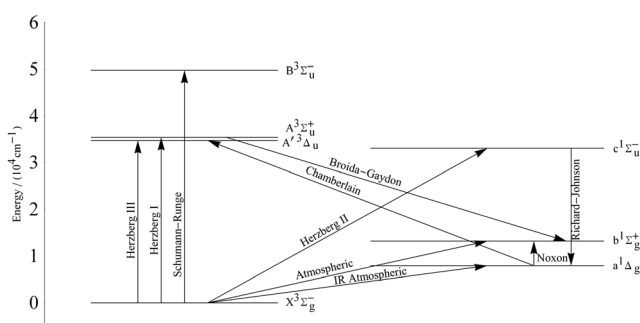


FIG. 1. Experimentally characterized band system of the $^{16}\text{O}_2$ molecule.

One of the primary goals of the project described herein is the collection and critical evaluation of all measured high-accuracy rovibronic transitions involving the bound states of the $^{16}\text{O}_2$ molecule. Since the reviews mentioned^{15,22,46,89,92–94,100,101} provide a comprehensive summary of the historically most important articles on the high-resolution spectroscopy of O_2 , we focus only on those sources which proved critical for building up our database of $^{16}\text{O}_2$ rovibronic transitions and energy levels. It is also important to emphasize that, although there are high-accuracy measurements related to the Rydberg states of $^{16}\text{O}_2$ (see, for example, the studies of Alberti *et al.*,¹⁷ Lewis *et al.*,⁵⁴ Ogawa *et al.*,²⁷ Katayama *et al.*,³⁰ Sur *et al.*,⁴⁸ Katsumata *et al.*,⁵¹ and England *et al.*⁵⁹), we collected the measured lines only up to the $\text{B}^3\Sigma_u^-$ state (see Fig. 1). The $\text{C}^3\Pi_g$ and $\text{d}^1\Pi_g$ states are considered to be the lowest Rydberg states.¹⁰⁰ In the present study, the validation, evaluation, and characterization of the measured high-resolution spectroscopic data of $^{16}\text{O}_2$ were executed using the MARVEL (Measured Active Rotational-Vibrational Energy Levels) protocol,^{108–112} based on the concept of spectroscopic networks (SNs).^{110,113,114} Since its inception a decade ago, the MARVEL algorithm and code was successfully employed to study the high-resolution spectra of several molecules, mostly of astronomical interest, including $^{12}\text{C}_2$,¹¹⁵ $^{48}\text{Ti}^{16}\text{O}$,¹¹⁶ $^{90}\text{Zr}^{16}\text{O}$,¹¹⁷ the H_3^+ , H_2D^+ , and D_2H^+ molecular ions,^{118,119} nine isotopologues of water,^{120–124} H_2^{32}S ,¹²⁵ three SO_2 isotopologues,¹²⁶ $^{12}\text{C}_2\text{H}_2$,¹²⁷ ammonia ($^{14}\text{NH}_3$),¹²⁸ and the parent ketene molecule.¹²⁹ Furthermore, the MARVEL energy levels of the water isotopologues were used for determining definitive ideal-gas thermochemical functions for H_2^{16}O ¹³⁰ and for heavy water and its three constituent isotopologues.¹³¹

During this study, we collected 30 671 rovibronic transitions among the lowest seven electronic states and determined 4279 empirical (MARVEL) energy levels for these states of $^{16}\text{O}_2$. The energy levels obtained, after supplementing them with the missing energy levels estimated through effective molecular Hamiltonians, are used to calculate the temperature-dependent ideal-gas partition function, $Q_{\text{int}}(T)$, of $^{16}\text{O}_2$ up to 5000 K. As is well known,¹³² all the other ideal-gas thermochemical quantities can be derived from $Q_{\text{int}}(T)$ and its first two moments; in this paper, we provide isobaric heat capacity ($C_p^\circ(T)$), entropy ($S^\circ(T)$), and (absolute) enthalpy ($H^\circ(T)$) values up to 5000 K. All thermochemical functions are reported, in 1 K increments, in the supplementary material. It is hoped that the high-quality data presented in this study will prove useful for a number of scientific and engineering applications, including the development of a new equation of state for O_2 to replace the previous equation, whose ideal-gas part was developed in 1982 by fitting to some handbook data.¹³⁴

Section 2 presents a methodological overview of how the MARVEL database of measured rovibronic transitions and empirical energy levels was created for the first seven electronic states of $^{16}\text{O}_2$. Section 3 reviews the large number of experimental sources included in the MARVEL database. Section 4 discusses the empirical MARVEL energy levels and provides a detailed comparison with their counterparts obtained earlier. Section 5 summarizes the creation of a hybrid database which contains both MARVEL and effective Hamiltonian energy levels for the lowest six electronic states. This hybrid database was employed for the determination of accurate ideal-gas thermochemical functions for $^{16}\text{O}_2$. Section 6 discusses the

internal partition function and the related thermochemical functions of $^{16}\text{O}_2$ up to 5000 K. Section 7 summarizes and concludes this study.

2. Methodological Details

2.1. MARVEL

The MARVEL approach^{108,110–114} enables the conversion of a set of assigned experimental rovibronic transitions to empirical rovibronic energy levels, with associated uncertainties propagated from the input transition data to the output energy levels. This conversion relies on the construction of an experimental SN¹¹³ from the measured and assigned transitions, facilitating an improved characterization of the high-resolution spectroscopic information.

2.2. Quantum numbers

The MARVEL algorithm needs uniquely labeled transitions in order to determine the empirical energy levels. In the case of the $^{16}\text{O}_2$ molecule, four pieces of information were used to label a rovibronic energy level: *state*, *v*, *J*, and *N* entries, where *state* defines the electronic state (see Fig. 1 and Table 1 for the list of the seven electronic states considered), *v* is the vibrational quantum number, *J* is the total angular momentum quantum number, while *N* represents the angular momentum quantum number without the consideration of electron spin. In the case of triplet states, *J* can have three values: *J* = *N* – 1 (F_3 component), *J* = *N* (F_2 component), and *J* = *N* + 1 (F_1 component), while in the case of singlet states, only the *J* = *N* component exists.

2.3. Electronic states of the $^{16}\text{O}_2$ molecule

The present MARVEL database contains rovibronic data corresponding to the following seven electronic states: $\text{X}^3\Sigma_g^-$, $\text{a}^1\Delta_g$, $\text{b}^1\Sigma_g^+$, $\text{c}^1\Sigma_g^-$, $\text{A}^1\Sigma_u^+$, $\text{A}'^3\Delta_u$, and $\text{B}^3\Sigma_u^-$. Table 1 summarizes the most important characteristics of the MARVEL rovibronic transitions collated during this study. It is important to note that although $^{16}\text{O}_2$ is a homonuclear diatomic molecule, more than 800 $\text{X}^3\Sigma_g^-$ – $\text{X}^3\Sigma_g^-$ transitions were measured experimentally. Table 2 lists 12 bands, most of which are named after their discoverers. Figure 1 depicts these bands on an energy scale. We note that the original papers reporting about the Richards–Johnson¹³⁶ and Broida–Gaydon¹³⁵ bands contain no high-accuracy transitions; therefore, these bands were left out from the MARVEL analysis.

3. Overview of the Literature

The full list of data sources used in the MARVEL analysis, along with some of their characteristics, is given in Table 3. As shown in Table 3, even the earliest experimental studies^{1–3} contain a lot of useful transitions, for example, 1526 of the 1733 lines measured in 1929 by Lochte-Holtgreven and Dieke¹ are confirmed, within their own accuracy, in the present study.

The present MARVEL database of $^{16}\text{O}_2$ contains 30 671 transition entries (Table 3). During this study, we departed from the usual way the input transitions subjected to a MARVEL analysis are handled. In all previous MARVEL studies,^{115–123,125–129} the input dataset contained only experimentally measured transitions with corresponding uncertainties. In this study, 24 376 transitions are measured lines but the rest of the 6295 transitions are what we call

TABLE 1. Electronic states of O₂ present in the MARVEL database collated during the present study, their notation, and the characterization of the experimental spectroscopic information available for them, where v_{\max} and J_{\max} stand for the maximum values of the vibrational and total angular momentum quantum numbers, respectively

State	MARVEL name	No. of energy levels	No. of transitions	v_{\max}	J_{\max}
X $^3\Sigma_g^-$	X3Sigmag	1479 ^a	23 734 ^a	21 ^a	86 ^a
a $^1\Delta_g$	a1Deltag	288 ^a	2237 ^a	10 ^a	48 ^a
b $^1\Sigma_g^+$	b1Sigmag	149 ^a	2765 ^a	15 ^a	46 ^a
c $^1\Sigma_u^+$	c1Sigmau	247	2016	19	30
A $^3\Sigma_u^+$	A3Sigmau	508	3969	12	33
A' $^3\Delta_u$ ($\Omega = 1$)	Ap3Deltau_1	271	1729	12	30
A' $^3\Delta_u$ ($\Omega = 2$)	Ap3Deltau_2	295	1815	12	33
A' $^3\Delta_u$ ($\Omega = 3$)	Ap3Deltau_3	251	2199	12	29
B $^3\Sigma_u^-$	B3Sigmau	798	8288	19	85

^aWithout artificial transitions. See Sec. 3 for the definition and use of artificial transitions.

artificial transitions. The artificial transitions have been created from the 14YuDrMi energy levels;⁹⁴ these transitions originate from (J, N) = (0, 1) on the ground electronic and vibrational state. We need to use these artificial transitions in order to get a large, connected SN for the lowest three electronic states. Without this connected “base component,” we could not determine the energy levels of high-lying electronic states. The Tag of artificial lines in the MARVEL transitions file, shown in the [supplementary material](#), begins with “A_-.”

The MARVEL database contains only high-resolution rovibronic lines and we deleted all measured lines which we could not reproduce within 0.5 cm⁻¹. Therefore, afterglow^{135,137-140} and nightglow^{141,142} spectra have been excluded from our analysis, since the uncertainties of these lines are usually larger than 0.5 cm⁻¹. There is only one partial exception, 06CoShSlHu.¹⁴² Of the five band systems, 06CoShSlHu¹⁴² contains, namely, Herzberg I ($A^3\Sigma_u^+ - X^3\Sigma_g^-$) Herzberg II ($c^1\Sigma_u^- - X^3\Sigma_g^-$), Chamberlain ($A'^3\Delta_u - a^1\Delta_g$), atmospheric ($b^1\Sigma_g^+ - X^3\Sigma_g^-$), and $c^1\Sigma_u^- - b^1\Sigma_g^+$, only the atmospheric lines were incorporated into the MARVEL database. We processed this source because (a) it contains a very large number of lines (2145 lines

for $^{16}\text{O}_2$) and (b) according to 14YuDrMi,⁹⁴ the uncertainties of the measured lines are as good as 0.1 cm⁻¹.

4. MARVEL Energy Levels

During this study, we determined, based on the 30 671 measured and artificial transitions, 4279 empirical rovibronic energy levels for $^{16}\text{O}_2$.

We are not aware of any truly high-accuracy first-principles energies for the $^{16}\text{O}_2$ molecule that could be used to check the empirical MARVEL energy levels derived during this study; therefore, we used spectroscopic constants available in the literature to confirm the MARVEL levels derived (see Figs. 2–7). Since we follow the convention of 14YuDrMi,⁹⁴ our lowest-energy level has (J, N) = (0, 1) with zero energy. Therefore, there is an about 1.0 cm⁻¹ shift between the MARVEL energy levels and the results of effective Hamiltonians. Consequently, we had to shift the energies corresponding to the effective Hamiltonians before comparing them with the MARVEL energy levels. Since the rovibrational energy levels of the lowest three

TABLE 2. Characterization of the experimental rovibronic transitions present in the MARVEL database^a

Band	Designation	No. of transitions
X $^3\Sigma_g^- - X^3\Sigma_g^-$		854 ^b
b $^1\Sigma_g^+ - X^3\Sigma_g^-$	Atmospheric	2672 ^b
a $^1\Delta_g - X^3\Sigma_g^-$	IR atmospheric	637 ^b
a $^1\Delta_g - a^1\Delta_g$		104
b $^1\Sigma_g^+ - a^1\Delta_g$	Noxon	93
B $^3\Sigma_u^- - X^3\Sigma_g^-$	Schumann–Runge	8288
c $^1\Sigma_u^- - X^3\Sigma_g^-$	Herzberg II	2016
A $^3\Sigma_u^+ - X^3\Sigma_g^-$	Herzberg I	3969
A' $^3\Delta_u$ ($\Omega = 1$) – X $^3\Sigma_g^-$	Herzberg III	1729
A' $^3\Delta_u$ ($\Omega = 2$) – X $^3\Sigma_g^-$	Herzberg III	1815
A' $^3\Delta_u$ ($\Omega = 3$) – X $^3\Sigma_g^-$	Herzberg III	900
A' $^3\Delta_u$ ($\Omega = 3$) – a $^1\Delta_g$	Chamberlain	1299

^aThe Broida–Gaydon¹³⁵ and the Richards–Johnson¹³⁶ bands (Fig. 1) measured in emission contain no rotational information, only transition band centers; thus, they were not considered for a MARVEL analysis.

^bWithout artificial transitions. See Sec. 3 for the definition of artificial transitions.

TABLE 3. Characteristics of data sources related to the $^{16}\text{O}_2$ molecule and analyzed during the present study, where A and V stand for the available and validated entries in a given source, respectively

Tag	Range/cm ⁻¹	A/V	Tag	Range/cm ⁻¹	A/V
75JoLe ²⁵	1.65–196.76	110/110	11GoRoTo ⁸⁶	12 847.19–15 927.81	221/221
82EnMi ³⁵	1.68–3.97	27/27	12MiWu ⁹⁰	12 849.57–13 339.20	59/59
81AmVe ³²	1.77–7 983.11	122/122	48BaHe ⁵	12 868.93–17 272.03	328/325
77LiGiHo ²⁸	1.79–2.12	10/10	17DrBeBrCi ⁹⁹	12 899.25–13 165.25	90/90
50BuAnSmGo ⁶	1.79–2.19	25/25	01BrCaBr ⁶⁸	12 926.78–13 165.25	80/80
05TrKoDoMa ⁷⁹	1.79–2.21	26/26	00YaCaWiCo ¹⁴³	12 941.65–13 093.65	19/19
54MiHi ¹³	1.79–3.96	24/24	69BuGr ²⁰	12 965.14–13 165.25	65/65
75ToMiHoEv ²⁶	1.82–128.95	19/19	90KaMoSa ⁴⁷	12 966.81–13 165.25	36/36
66WeMi ¹⁶	1.82–2.19	9/9	99ScLe ¹⁴⁴	12 977.10–13 165.25	67/67
68McGo ¹⁸	1.88–16.25	7/7	08RoHoMaYe ⁸⁰	12 977.11–13 114.10	32/32
51GoSt ⁹	1.88–2.08	8/8	08Robichaud ¹⁴⁵	12 977.11–13 114.10	32/32
74AmHi ²³	1.93–2.09	9/9	27DiBa ¹⁴⁶	12 977.11–17 272.08	197/196
61ZiMi ¹⁴	1.95–2.18	12/12	08PrHaKePo ⁸¹	13 010.81–13 165.17	112/102
A_14YuDrMi ⁹⁴	2.08–41 258.89	3503/3503	00BrPl ⁶⁵	13 031.39–13 160.81	44/43
51AnJoGo ⁸	3.96–3.96	1/1	A_14YuDrMi_b ⁹⁴	13 122.01–41 252.34	916/916
04TrGoPaKo ⁷⁶	3.96–3.96	1/1	80Brault ³¹	13 179.92–13 280.03	8/8
95CoOkOh ⁵⁵	8.40–14.00	3/3	16DoWoMaCy ⁹⁷	14 438.17–14 557.98	18/18
83CaEsFa ³⁶	8.51–11.34	2/2	14WoCyMaDo ⁹⁵	14 440.00–14 522.78	20/20
85HiChReCo ³⁸	8.51–28.34	8/8	17BiWoMoAb ⁹⁸	14 502.82–14 502.82	1/1
81ScSaEvRa ³⁴	11.34–25.51	5/5	15DoWoMaCy ⁹⁶	14 531.02–14 550.02	11/11
03GoKr ⁷²	12.29–37.38	8/8	12DoWoLiCy ⁸⁸	14 546.00–14 557.98	12/12
02KrGoMaSe ⁷⁰	14.17–14.17	1/1	99NaNaUb ⁶²	15 766.52–15 927.82	49/49
10DrYuMiMu ⁸³	14.17–62.38	9/9	11Slanger ⁸⁷	16 262.61–29 680.60	1299/1292
92BrRiNi ⁴⁹	14.30–117.58	30/30	98BiCa ⁶⁰	17 133.71–17 272.04	43/43
12DrGuYuMi ⁸⁹	16.80–90.07	12/12	99NaUb ⁶³	17 148.14–17 272.05	42/42
87ZiMi ⁴⁵	25.81–83.47	5/5	68Degen ¹⁹	20 773.61–22 269.73	59/56
96PaNoStZi ⁵⁸	50.87–83.47	2/2	29LoDi ¹	22 453.55–32 205.48	1733/1526
87NiVa ⁴⁴	1 324.37–1 479.08	74/62	93CiRa ⁵²	24 700.26–271 085.23	511/489
74FlRa ²⁴	1 420.11–1 686.44	39/39	50Feast ⁷	31 991.80–40 298.00	913/673
92RoMiSaBe ⁵⁰	1 432.81–1 696.13	213/213	86Ramsay ⁴³	33 389.81–40 854.53	513/513
03BrBe ⁷¹	1 445.39–1 686.45	61/61	01MeJeCoCa ⁶⁹	34 014.09–41 260.53	4860/4801
81EdLoNaTh ³³	1 457.88–1 656.51	70/70	86BoBoRa ⁴⁰	34 910.42–41 156.65	965/941
77LoBe ²⁹	1 494.63–1 614.63	84/84	52Herzberg ¹⁰	35 647.99–41 172.66	606/591
96MiLaFa ⁵⁷	1 530.25–1 530.36	3/3	86CoRa ⁴¹	35 792.53–40 989.33	834/834
86FiKrRaVe ⁴²	5 132.22–5 319.00	48/48	53Herzberg ¹¹	36 604.22–39 355.78	294/274
04GuOwBaOk ⁷⁴	5 229.37–5 238.34	8/8	99YoEsPaTh ⁶⁴	36 604.64–40 862.40	427/423
09FoCeMaVe ⁸²	6 564.97–6 662.68	29/29	85KeWa ³⁹	37 079.57–39 001.67	53/53
04WiGuOwBa ⁷⁷	6 630.99–6 642.95	8/8	00YoEsPaTh ⁶⁷	37 282.82–40 949.90	1062/1049
10LeKaGoRo ⁸⁵	7 648.94–7 915.86	199/199	94YoMuEsSu ⁵³	37 630.00–41 167.67	756/752
10GoKaCaTo ⁸⁴	7 667.89–8 114.70	112/112	05HaDuUb ⁷⁸	48 976.14–50 714.65	188/187
00ChLeOg ⁶⁶	7 732.86–15 927.80	277/277	84YoFrPa ³⁷	49 018.07–56 851.63	1594/1537
47HeHe ⁴	7 809.94–9 451.75	131/129	70AcBi ²¹	49 139.32–56 085.70	562/528
A_14YuDrMi_a ⁹⁴	7 892.02–41 234.93	1876/1876	34CuHe ²	49 908.13–52 208.92	134/73
13DrYuElCr ⁹³	9 973.21–13 165.25	201/201	96ChYoEsPa ⁵⁶	50 523.39–55 295.10	1398/1370
06CoShSIHu ¹⁴²	10 011.33–15 715.71	586/583	35KrBa ⁵	51 830.00–56 550.00	243/8
04LeKjHoWi ⁷⁵	12 847.17–13 010.62	71/71	54BrHe ¹²	55 126.81–557 664.40	574/551
12ObObOb ⁹¹	12 847.19–13 010.60	65/65	03MaChLeYo ⁷³	55 400.80–56 851.57	438/427

electronic states ($X^3\Sigma_g^-$, $a^1\Delta_g$, and $b^1\Sigma_g^+$) of $^{16}\text{O}_2$ in the MARVEL set are confirmed by 14YuDrMi,⁹⁴ a source that provides probably the best energy levels available in the literature for these states, an analysis of these energy levels is not pursued.

For the energy levels of the next electronic state, the $c^1\Sigma_u^-$ state, we used the spectroscopic constants found in 86Ramsay,⁴³ 99JeMeCoCa,¹⁴⁷ and 99YoEsPaTh.⁶⁴ Figure 2 shows the differences between the MARVEL levels and these earlier results. As shown in

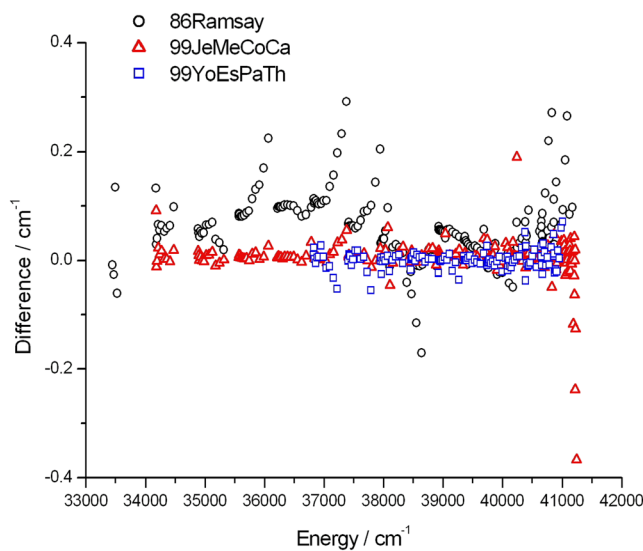


FIG. 2. Differences between the empirical (MARVEL) energy levels of this study and the earlier literature results of 86Ramsay,⁴³ 99JeMeCoCa,¹⁴⁷ and 99YoEsPaTh,⁶⁴ all related to the $c\ 1\Sigma_u^-$ electronic state of $^{16}\text{O}_2$.

Fig. 2, considerable scatter characterizes the previous results, especially those of 86Ramsay.⁴³

For the energy levels of the $A\ 3\Sigma_u^+$ state, we used the molecular constants found in 86BoBoRa,⁴⁰ 94YoMuEsSu,⁵³ and 99JeMeCoCa.¹⁴⁷ Additionally, we used the term expressions of 52Herzberg¹⁰ to compute the F_1 , F_2 , and F_3 values of the $A\ 3\Sigma_u^+$ state. Figure 3 shows the differences between the empirical MARVEL energy levels and the earlier literature

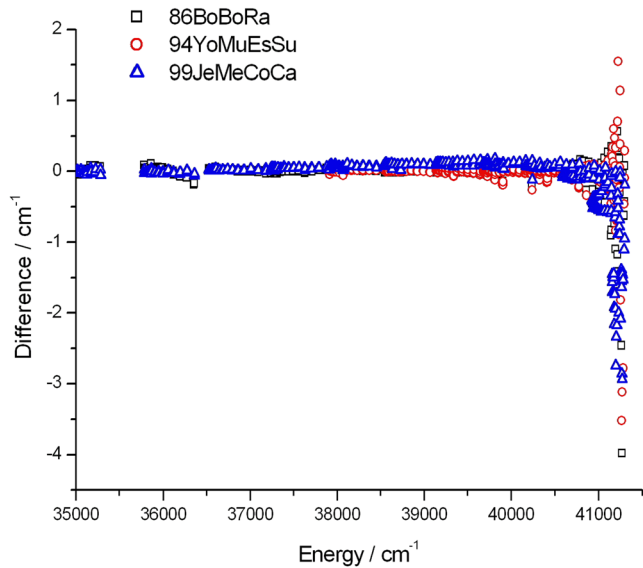


FIG. 3. Differences between the empirical (MARVEL) energy levels and the earlier literature results of 86BoBoRa,⁴⁰ 94YoMuEsSu,⁵³ and 99JeMeCoCa,¹⁴⁷ all related to the $A\ 3\Sigma_u^+$ electronic state of $^{16}\text{O}_2$.

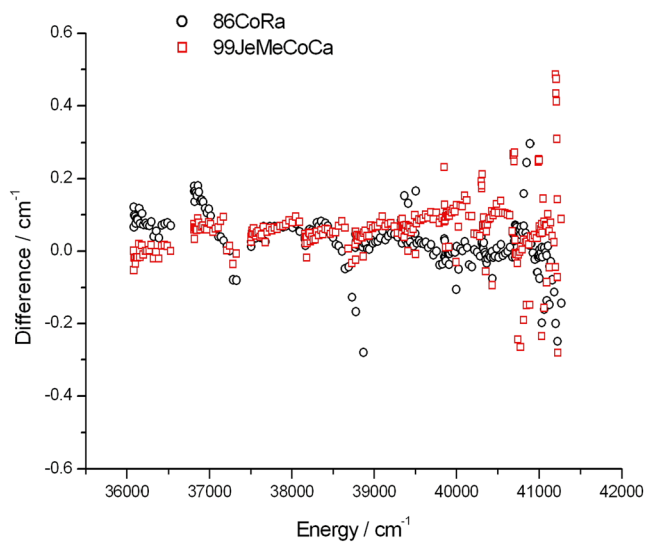


FIG. 4. Differences between the empirical (MARVEL) energy levels and the earlier results of 86CoRa⁴¹ and 99JeMeCoCa¹⁴⁷ on the $A'\ 3\Delta_u$ ($\Omega = 1$) state of $^{16}\text{O}_2$.

results. The spectroscopic parameters for the $\nu \geq 11$ states, close to the first dissociation limit, appear to be rather uncertain, causing unusually large deviations for these energy levels.

For the energy levels of the close-lying $A'\ 3\Delta_u$ state, we used the spectroscopic constants found in 86CoRa⁴¹ and 99JeMeCoCa.¹⁴⁷ We used the effective Hamiltonians of Refs. 148 and 149 to compute the energy values of the ${}^3\Delta_{1u}(F_1)$, ${}^3\Delta_{2u}(F_2)$, and ${}^3\Delta_{3u}(F_3)$ states. Figures 4, 5, and 6 show the differences between the MARVEL energy levels and the earlier results for the $\Omega = 1$, $\Omega = 2$, and $\Omega = 3$ states,

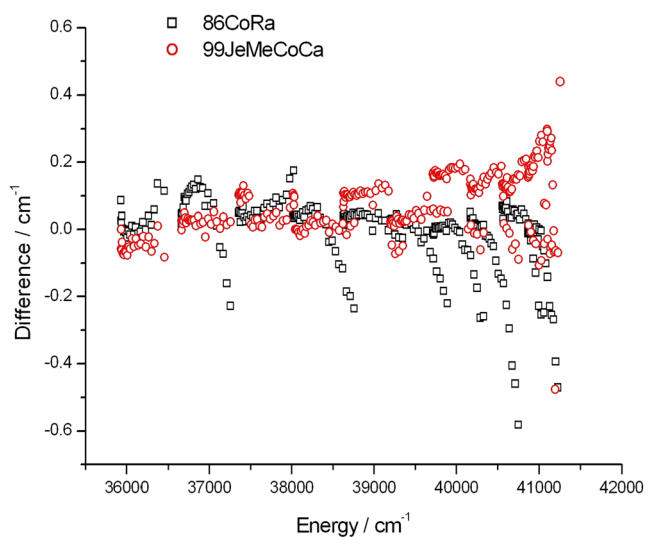


FIG. 5. Differences between the empirical (MARVEL) energy levels and the earlier results of 86CoRa⁴¹ and 99JeMeCoCa¹⁴⁷ on the $A'\ 3\Delta_u$ ($\Omega = 2$) state of $^{16}\text{O}_2$.

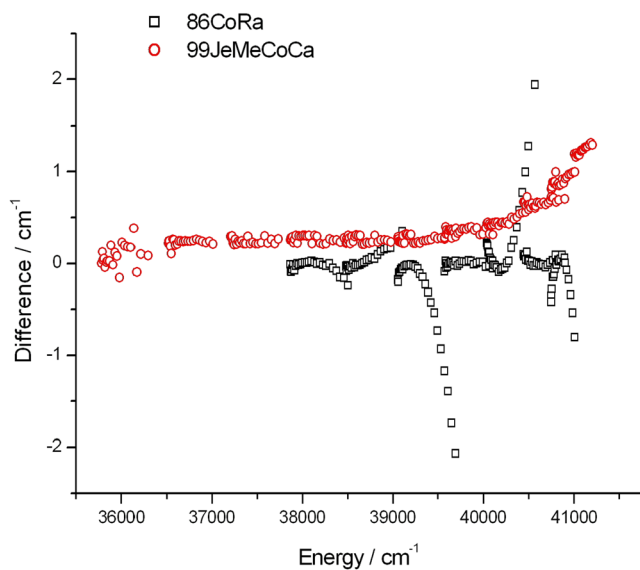


FIG. 6. Differences between the empirical (MARVEL) energy levels and the earlier results of 86CoRa⁴¹ and 99JeMeCoCa¹⁴⁷ on the A' $^3\Delta_u$ ($\Omega = 3$) state of $^{16}\text{O}_2$.

respectively. We note that the spectroscopic parameters for the $\Omega = 3$ states are the worst determined, causing large deviations for these energy levels.

For the energy levels of the B $^3\Sigma_u^-$ state, we employed the spectroscopic constants of 86ChYoPaFr,¹⁵⁰ 96ChYoEsPa,⁵⁶ 03MaChLeYo,⁷³ and 05HaDuUb.⁷⁸ We used the term expressions of 52Herzberg¹⁰ to compute the F_1 , F_2 , and F_3 values of the B $^3\Sigma_u^-$ state. Figure 7 shows the deviations between the empirical MARVEL energy levels and the earlier results.^{56,73,78,150}

Overall, it is clear that the empirical MARVEL energy levels provide an outstanding, and at the same time self-consistent, representation of the existing high-resolution spectroscopic studies of $^{16}\text{O}_2$ for the lowest seven electronic states and that issues with certain experimental data are raised as a result. While the MARVEL procedure could validate most of the measured transitions below about $13\,000\text{ cm}^{-1}$, above this threshold there are certain sources, including 29LoDi,¹ 50Feast,⁷ and especially 35KrBa,³ where a relatively large number of published transitions could not be validated. Finally, we express our hope that future accurate measurements will help to eliminate the great majority, if not all, of the artificial transitions that had to be employed during the present study.

5. The Hybrid Dataset

Besides creating the MARVEL database of $^{16}\text{O}_2$ transitions and the related empirical energy levels, the second principal aim of the present study has been the determination of accurate ideal-gas thermochemical functions for the $^{16}\text{O}_2$ molecule. To apply the direct-summation technique [see Eq. (1)] for this purpose, we need the complete set of rovibronic energy levels to as high energy as feasible.

As mentioned earlier, we are not aware of any high-accuracy *ab initio* results for the $^{16}\text{O}_2$ molecule; therefore, during the augmentation of the incomplete set of rovibronic MARVEL energies, we

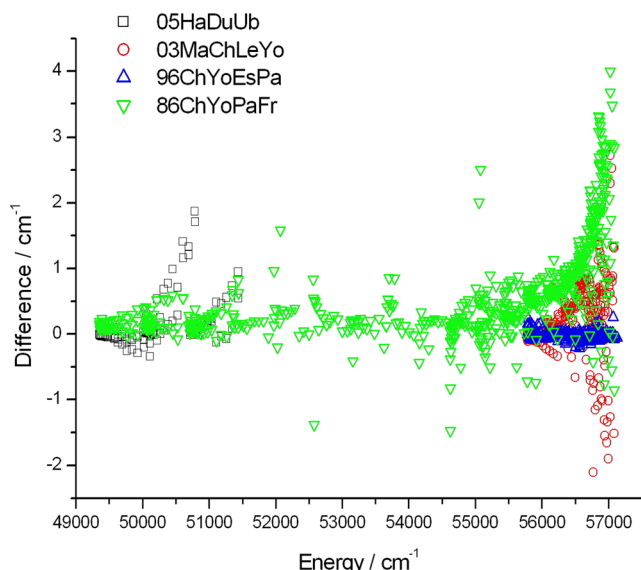


FIG. 7. Differences between the empirical (MARVEL) energy levels and the earlier literature results of 05HaDuUb,⁷⁸ 03MaChLeYo,⁷³ 96ChYoEsPa,⁵⁶ and 86ChYoPaFr¹⁵⁰ related to the B $^3\Sigma_u^-$ electronic state.

must rely on energies based on effective Hamiltonians. We call the augmented (complete) set of rovibronic energies a hybrid dataset.

It is important to emphasize that our aim was to create a complete set of energy levels for the $^{16}\text{O}_2$ molecule and not to compute the best effective Hamiltonian energy levels. Therefore, we used the most complete set of spectroscopic constants and not necessarily the best individual parameters. For example, it is feasible that the parameters of 00YoEsPaTh⁶⁷ provide better energy values for some of the vibrational states of the A' $^3\Delta_u$ electronic state than those of 01MeJeCoCa,⁶⁹ but the latter source provides a more complete set of spectroscopic constants; thus, we used the 01MeJeCoCa⁶⁹ source exclusively. Furthermore, since our aim is not to reach spectroscopic accuracy with the effective Hamiltonian energies, just completeness, we neglected the coupling among the electronic states in our calculations.

To create the hybrid dataset, we replaced the effective Hamiltonian energy levels of the first six electronic states of $^{16}\text{O}_2$ with MARVEL energies whenever possible and in this way we obtain the most accurate and at the same time complete database for the $^{16}\text{O}_2$ molecule (note that we neglected the rovibrational levels of the B $^3\Sigma_u^-$ state during the thermochemical calculations, see below). The molecular constants of 14YuDrMi⁹⁴ were used to calculate the energy levels of the X $^3\Sigma_g^-$, the a $^1\Delta_g$, and the b $^1\Sigma_g^+$ states up to the dissociation limit. Note that 14YuDrMi⁹⁴ uses the powers of $[J(J+1) - \Omega^2]$ instead of $[J(J+1)]$ in the case of the a $^1\Delta_g$ state. The supplementary material of Ref. 94 contains the molecular constants up to $\nu = 35, 29$, and 29 for the X $^3\Sigma_g^-$, a $^1\Delta_g$, and b $^1\Sigma_g^+$ states, respectively. We used the spectroscopic constants of 01MeJeCoCa⁶⁹ to determine the rovibrational energy levels of the c $^1\Sigma_u^-$, the A $^3\Sigma_u^+$, and the A' $^3\Delta_u$ states. We employed the calculated spectroscopic parameters of 88SiCo⁴⁶ for $\nu = 0$ and the parameters of 86Ramsay⁴³ for $\nu = 1$ of the c $^1\Sigma_u^-$ state. Furthermore, the calculated spectroscopic parameters of 88SiCo⁴⁶

were utilized to calculate the $\nu = 0$ and 1 energy levels of the $A' ^3\Delta_u$ state. The dissociation energy is $41\,260 \pm 15\text{ cm}^{-1}$ for the $O(^3P_g) + O(^3P_g)$ dissociation channel^{151,152} (i.e., for the six electronic states considered: $X ^3\Sigma_g^-$, $a ^1\Delta_g$, $b ^1\Sigma_g^+$, $c ^1\Sigma_u^-$, $A ^3\Sigma_u^+$, and $A' ^3\Delta_u$).

In order to determine the uncertainties of the thermochemical functions, it is essential that each rovibronic energy level has its own uncertainty. We employ the extremely conservative expression of $0.5 \times N\text{ cm}^{-1}$ to estimate the uncertainties of the effective Hamiltonian energy levels, where N is the angular momentum quantum number without the consideration of electron spin. For lower N values, MARVEL energy levels with well-defined uncertainties are available (these energy levels also allow the testing of the $0.5 \times N$ estimate); thus, we only need to estimate the uncertainties this way for energy levels characterized by large N values.

The hybrid dataset contains 15 946 energy levels. This means that we added 11 667 effective Hamiltonian energy levels to the MARVEL set, essentially quadrupling the original set of 4279 empirical rovibronic energy levels. In the hybrid database, which can be found in the [supplementary material](#), each energy level has a label M (MARVEL level) or H (effective Hamiltonian level), indicating the level's origin. While the empirical MARVEL energy levels of the $B ^3\Sigma_u^-$ state have not been involved in the final thermochemical calculations, for the sake of completeness, they are present in the hybrid database of the [supplementary material](#).

6. Ideal-Gas Partition and Thermochemical Functions

The direct summation technique, represented by the expressions

$$Q_{\text{int}}(T) = \sum_i d_i \exp\left(\frac{-c_2 E_i}{T}\right), \quad (1)$$

$$Q'_{\text{int}} = T \frac{dQ_{\text{int}}}{dT} = \sum_i d_i \left(\frac{c_2 E_i}{T}\right) \exp\left(\frac{-c_2 E_i}{T}\right), \quad (2)$$

and

$$Q''_{\text{int}} = T^2 \frac{d^2 Q_{\text{int}}}{dT^2} + 2Q'_{\text{int}} = \sum_i d_i \left(\frac{c_2 E_i}{T}\right)^2 \exp\left(\frac{-c_2 E_i}{T}\right), \quad (3)$$

was used in this study to calculate the temperature-dependent internal partition function [Eq. (1)] and its first two moments [Eqs. (2) and (3), all unitless quantities] of the $^{16}\text{O}_2$ molecule, where c_2 is the second radiation constant ($c_2 = 1.438\,777\,36(83)\text{ cm K}$), and E_i is the value (in cm^{-1}) and d_i is the degeneracy factor of the i th rovibronic energy level. For the expressions for deriving further thermochemical functions from $Q_{\text{int}}(T)$, we refer the reader to a standard textbook¹⁵² and Ref. 130.

The two main sources of the uncertainties of thermochemical functions calculated via the direct-summation technique are as follows:¹³⁰ (a) the uncertainty about the number of energy levels (uncertainty about the energy density) and (b) uncertainties of the rovibronic energy levels used to determine the partition function.

Checking the convergence of the partition function at a given temperature is somewhat difficult because its value grows monotonically as more and more energy levels are considered in the direct sum. In other words, it is impossible to calculate the possible contribution of missing states (which were skipped from the direct sum) since their number and their energy values are unknown.

TABLE 4. Number of energy levels and the average rotational quantum number (J) in different energy regions

Region/cm ⁻¹	Number of energy levels	Average J value
37 000–38 000	935	55
38 000–39 000	1099	53
39 000–40 000	1266	54
40 000–41 000	1597	51

Nevertheless, we can easily obtain an upper bound for this possible contribution using the following inequality:

$$\sum_{i \in \{E_i > 41000\}} (2J_i + 1) \exp\left(\frac{-c_2 E_i}{T}\right) < n_{\text{missing}} (2J_{\text{avg}} + 1) \\ \times \exp\left(\frac{-c_2 41000}{T}\right) = Q^{\text{missing}}. \quad (4)$$

We chose the $41\,000\text{ cm}^{-1}$ limit in Eq. (4) because the hybrid dataset can safely be considered complete up to this energy value. To estimate the number of missing energy levels (n_{missing}) and the average J value (J_{avg}), we checked the number of energy levels and the average J value in a few known regions. Using the values of Table 4, we chose $n_{\text{missing}} = 10\,000$ and $J_{\text{avg}} = 60$. Obviously, $n_{\text{missing}} = 10\,000$ is a gross overestimation, but using this large n_{missing} value, we can definitely find the temperature from where contribution of the unbound rovibrational states¹³⁰ or the higher electronic states becomes non-negligible. Figure 8 shows the contribution of Q^{missing} and its second moment in % up to 5000 K. If the aim is to determine the isobaric heat capacity, $C_p^o(T)$, within 1.0%, then the maximum temperature we can reach with this criterion is about 5000 K. Another good test of checking the convergence of the partition function is to exclude the energy levels of the $B ^3\Sigma_u^-$ state from the calculation. Comparing the thermochemical functions with and without the 2168

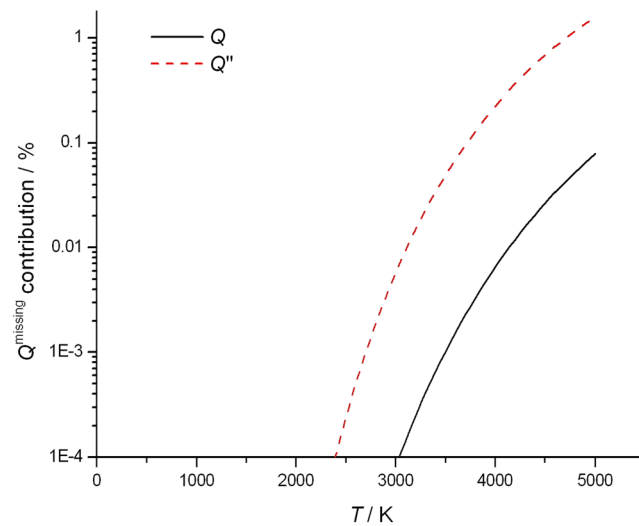


FIG. 8. The contribution of Q^{missing} (solid line) and Q''^{missing} (dashed line) in % at different temperatures.

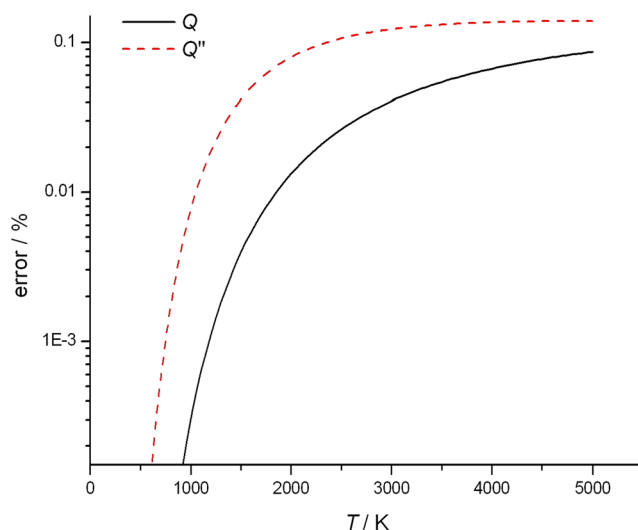


FIG. 9. Uncertainty of the partition function (solid line) and its second moment (dashed line) using the “two extrema” method.

MARVEL and effective Hamiltonian energy levels of the $B\ ^3\Sigma_u^-$ state, we found that the effect of the $B\ ^3\Sigma_u^-$ state is less than 0.01% for C_p^o (5000 K).

We used the “two extrema” method¹³⁰ to determine the uncertainty of the partition function caused by the uncertainties of the energy levels. According to Fig. 9, the maximum value of this uncertainty is about 0.1% (increasing monotonically up to 5000 K, it remains below 0.01% below 2000 K), so the uncertainty about the number of energy levels determines the final uncertainties at

higher temperatures; therefore, we calculate the thermochemical functions up to 5000 K. The final uncertainty of the partition function is given by combining the two uncertainties described. We consider our uncertainty estimates as representations of 95% uncertainty intervals. Table 5 shows the values of $Q_{int}(T)$ at selected temperatures.

Next, we compare our internal partition function to those of earlier studies, 14YuDrMi,⁹⁴ 48Woolley,¹⁵³ TIPS,¹⁵⁴ ESA (European Space Agency),¹⁵² 16BaCo,¹⁵⁵ 85RoMaBe,¹⁵⁶ and 81Irwin.¹⁵⁷ As expected, all sources result in similar $Q_{int}(T)$ values at lower temperatures (say, up to 1000 K). At higher temperatures, there are a few interesting discrepancies worth analysing one after the other.

First, the agreement between this study and that of 14YuDrMi⁹⁴ is excellent up to room temperature, where the latter data terminate. This is expected as a considerable number of energy levels is common to the two studies (*vide supra*).

Second, although 48Woolley¹⁵³ provided seemingly excellent Dunham polynomial coefficients to evaluate the energy levels of four electronic states of $^{16}\text{O}_2$, at the end, a simple polynomial expression was derived for the partition function and the other thermochemical functions. The agreement between our results and those of 48Woolley is excellent all the way to 5000 K, a very pleasing result, especially considering the year the 48Woolley¹⁵³ thermochemical data were generated.

Third, the TIPS (total internal partition sums)¹⁵⁴ data deviate more and more from those of the present study as the temperature increases (the agreement is perfect up to room temperature). During generation of the TIPS data,¹⁵⁴ only the three lowest electronic states ($X\ ^3\Sigma_g^-$, $a\ ^1\Delta_g$, and $b\ ^1\Sigma_g^+$) were considered. This fact alone, however, does not explain the observation of too low TIPS values, as the contribution of higher electronic states becomes significant only above about 2000 K. The observed discrepancy is

TABLE 5. Temperature-dependent ideal-gas internal partition function with estimated uncertainties in parentheses (in units of the last quoted decimal place), $Q_{int}(T)$, of the $^{16}\text{O}_2$ molecule at selected temperatures obtained by different sources

T/K	This work	14YuDrMi ⁹⁴	48Woolley ¹⁵³	TIPS ¹⁵⁴	ESA ¹⁵²	16BaCo ¹⁵⁵	85RoMaBe ¹⁵⁶	81Irwin ¹⁵⁷
9.375	7.871 293(6)	7.8713						
18.750	14.514 942(6)	14.5149						
37.5	28.034 485(5)	28.0345						
75	55.197 844(5)	55.1979		55.198				
100	73.327 201(5)		73.344	73.327	73.45	76.1289		
150	109.604 940(5)	109.6050		109.60	109.9			
200	145.901 548(5)		145.931	145.90	146.4	148.678		
296	215.736 329(5)	215.7364		215.73				
300	218.656 197(5)	218.6562	218.705	218.65	219.6	221.427		
400	292.304 797(5)		292.374	292.25	293.7			
600	447.566 16(1)		447.681	446.18	449.8			
800	620.726 8(3)		620.90	612.55	623.9			
1000	816.661(3)		816.91	791.00	820.9	819.779	817.517	813.309
1500	1 418.98(7)		1 419.12	1276.7		1 422.63	1 419.119	1 411.206
2000	2 195.1(4)		2 195.78	1801.4	2 207	2 199.51	2 191.565	2 179.893
2500	3 161(1)		3 162.15	2357.2			3 151.247	3 134.923
3000	4 337(2)		4 337.94	2944.1	4 362	4 344.27	4 316.783	4 294.705
4000	7 406(6)		7 404.10	4219.3	7 452	7 418.70	7 346.694	7 308.399
5000	11 583(10)		11 569.8	5638.6	11 660	11 607.0	11 455.135	11 388.158

TABLE 6. Ideal-gas enthalpy with estimated uncertainties in parentheses (in units of the last quoted decimal place), $H^\circ(T)$ (in J mol^{-1}), of the $^{16}\text{O}_2$ molecule at selected temperatures T obtained by different sources

T/K	This work	48Woolley ^{153 a}	63McBride ¹⁵⁸	ESA ¹⁵²	Gurvich ¹⁵¹	JANAF ¹⁵⁹
100	2 901.060 66(6)	2 901.085	2 901.60	2 905	2 901	2 901
200	5 812.490 35(6)	5 812.516	5 812.83	5 816	5 812	5 812
300	8 734.552 42(6)	8 734.594	8 734.94	8 738	8 735	8 734
400	11 705.819 35(5)	11 705.921	11 706.40	11 710	11 706	11 705
500	14 764.792 96(4)	14 764.991	14 765.30	14 770	14 765	14 764
1000	31 385.1(2)	31 385.703	31 386.70	31 390	31 386	31 383
1500	49 288(3)	49 287.587	49 289.20		49 290	49 279
2000	67 880(10)	67 877.830	67 878.30	67 890	67 882	67 855
2500	87 061(18)	87 054.046	87 052.30		87 063	87 008
3000	106 796(26)	106 777.120	106 776	106 800	106 797	106 693
4000	147 673(25)	147 564.932	147 611	147 700	147 680	147 385
5000	189 918(116)	189 570.366	189 798	190 100	190 040	189 429

^aWe used Eq. (7) of 48Woolley¹⁵³ to compute $H^\circ(T)$.

traced to the fact that TIPS¹⁵⁴ worked with a subset of energy levels (high- ν states were not considered) needed to obtain a converged partition function.

Fourth, ESA¹⁵² uses anharmonic-oscillator and non-rigid-rotor expressions to calculate the energy levels. This seems to explain why the differences between this study and ESA's results become slightly larger at higher temperatures. It is also of interest to note that, somewhat uncharacteristically, ESA *overestimates* the partition function, even at the lowest temperatures.

Fifth, 16BaCo¹⁵⁵ considered spin-orbit coupling in their energy calculations; therefore, their results are better than the ones from ESA (except at 100 K, where 16BaCo,¹⁵⁵ for an unclear reason, significantly overestimates the partition function).

Sixth, it is interesting to note that 85RoMaBe,¹⁵⁶ a study whose aim was to determine accurate partition functions for astrophysically important molecules from 1000 K to 5000 K, significantly underestimates the true partition function above 2000 K. This is more surprising as at 1000 and 1500 K, the partition function has too high values. The reason behind this behavior is not transparent to us.

Finally, 81Irwin¹⁵⁷ similarly underestimates the values of the partition function; the differences between our results and those of 81Irwin are surprisingly large.

Table 6 contains the ideal-gas enthalpy, $H^\circ(T)$ (in J mol^{-1}), as a function of temperature. It can be seen that at lower temperatures, most of the sources result in very similar values, but above 2000 K, the differences might be a few hundred J mol^{-1} .

Table 7 contains the isobaric heat capacity, $C_p^\circ(T)$, as a function of temperature, as well as a comparison to the best previous results obtained by 48Woolley,¹⁵³ 63McBride,¹⁵⁸ 73JaStMy,¹⁶⁰ 82WaEwSc,¹³⁴ JANAF,¹⁵⁹ and Gurvich.¹⁵¹ Since the value of the heat capacity changes in a narrow range ($29\text{--}43 \text{ J mol}^{-1} \text{ K}^{-1}$), the differences between the sources at higher temperatures are not particularly significant (though considerably larger than the uncertainties of this work). Note also that the Gurvich¹⁵¹ data are slightly closer to the present definitive values than are those of JANAF.¹⁵⁹

The partition function and its first two moments, as well as the $C_p^\circ(T)$, $S^\circ(T)$, and $H^\circ(T)$ thermochemical functions, are listed in 1 K increments in the [supplementary material](#).

TABLE 7. Ideal-gas isobaric heat capacity with estimated uncertainties in parentheses (in units of the last quoted decimal place), $C_p^\circ(T)$ (in $\text{J mol}^{-1} \text{ K}^{-1}$), of the $^{16}\text{O}_2$ molecule at selected temperatures T obtained by different sources

T/K	This work	48Woolley ^{153 a}	JANAF ¹⁵⁹	Gurvich ¹⁵¹	73JaStMy ¹⁶⁰	82WaEwSc ¹³⁴	63McBride ¹⁵⁸
100	29.111 881(1)	29.112	29.106	29.112	29.110	29.114	29.1194
200	29.127 443(1)	29.127	29.126	29.127	29.129	29.127	29.1269
300	29.386 489(1)	29.387	29.385	29.387	29.386	29.385	29.3872
400	30.107 318(1)	30.108	30.106	30.108	30.107	30.107	30.1085
500	31.091 863(3)	31.091	31.091	31.093	31.094	31.093	31.0934
1000	34.877(2)	34.878	34.870	34.880	34.879	34.878	34.8787
1500	36.565(10)	36.563	36.544	36.566	36.574	36.576	36.5623
2000	37.78(2)	37.777	37.741	37.783	37.804	37.822	37.7732
2500	38.93(2)	38.927	38.856	38.929		39.005	38.9133
3000	39.99(2)	39.952	39.864	39.986		40.104	39.9605
4000	41.66(3)	41.499	41.421	41.695		41.947	41.6028
5000	42.7(3)	42.446	42.675	43.009			42.6998

^aWe used Eq. (7) of 48Woolley¹⁵³ to compute $C_p^\circ(T)$.

7. Summary and Conclusions

All publicly available, assigned, and experimentally measured rovibronic transitions of the $^{16}\text{O}_2$ molecule have been collated into a single database. Using the collected 30 671 transitions, of which only 1119 could not be validated, and the MARVEL protocol, we determined 4279 empirical rovibronic energy levels. The measured transitions, and thus the empirical energy levels, span 7 electronic states ($\text{X}^3\Sigma_g^-$, $\text{a}^1\Delta_g$, $\text{b}^1\Sigma_g^+$, $\text{c}^1\Sigma_u^-$, $\text{A}^3\Sigma_u^+$, $\text{A}'^3\Delta_u$, and $\text{B}^3\Sigma_u^-$, see Fig. 1) in the 1.65–55 400.80 cm $^{-1}$ range.

The rovibronic energies derived allow the accurate determination of the temperature-dependent ideal-gas internal partition function, $Q_{\text{int}}(T)$, of the $^{16}\text{O}_2$ molecule through the direct-summation technique. At lower temperatures, this process provides the ultimate partition function as it uses the highly accurate empirical (MARVEL) energy levels. At higher temperatures, above about 1000 K, the completeness of the energy level set determines the true accuracy of the partition function. Therefore, the MARVEL database had to be supplemented with effective Hamiltonian energy levels up to the first dissociation limit. The final, hybrid dataset thus obtained contains 15 946 energy levels, corresponding to the lowest seven electronic states. This means that about 25% of the bound energy levels of $^{16}\text{O}_2$ below the first dissociation limit are known experimentally. Using the hybrid dataset, the internal partition function and its first two moments (and the corresponding uncertainties) were calculated up to 5000 K, within a 1.0% uncertainty even at the highest temperature. Using the partition function and its first two moments, very accurate thermochemical functions, including the ideal-gas isobaric heat capacity, $C_p^o(T)$, the enthalpy, $H^o(T)$, and the entropy, $S^o(T)$ were determined. Comparison of our results with determinations available in the literature allows the identification of limitations of some of the previous studies.

This study proved once again that the best way to determine highly accurate (ideal-gas) partition functions and the related thermochemical functions involves the use of a combined set of experimental and accurately computed/calculated energy levels and the direct-summation technique. The partition function and its first two moments, as well as the $C_p^o(T)$, $S^o(T)$, and $H^o(T)$ thermochemical functions determined as part of this study, are listed in 1 K increments in the [supplementary material](#).

As to the other dioxygen isotopologues, there are too few measured lines to perform a comprehensive MARVEL analysis based on them. 14YuDrMi⁹⁴ collected and successfully analyzed 1523, 991, 1657, 973, and 912 measured lines for $^{16}\text{O}^{17}\text{O}$, $^{16}\text{O}^{18}\text{O}$, $^{17}\text{O}_2$, $^{17}\text{O}^{18}\text{O}$, and $^{18}\text{O}_2$, respectively. Due to the small number of observed lines, we decided not to perform a MARVEL analysis, since (a) the measured lines probably do not create a well-connected component, so only a relatively few MARVEL energy levels corresponding to the principal component of the measured spectroscopic network could be determined for the given isotopologue and (b) we cannot give extra information about the energy levels of these isotopologues compared to 14YuDrMi.⁹⁴

Finally, it is the privilege of the senior authors to note that the majority of the data collection and data evaluation work was performed by 16- and 17-year-old high-school students, involved in a pilot education study in Hungary.

8. Supplementary Material

See [supplementary material](#) for the hybrid energy levels (HybridEnergyLevels.txt), the collected experimental transitions

(MARVEL_transitions.txt), the computed partition functions (PartitionFunctions.txt), and the calculated thermochemical functions (ThermochemicalFunctions.txt) of the $^{16}\text{O}_2$ molecule.

Acknowledgments

A.G.C. is grateful for the financial support received from NKFIH through Grant No. K119658. Our research also received support from Grant Nos. VEKOP-2.3.2-16-2017-00014 and EFOP-3.4.4-16-2017-00006, supported by the European Union and the State of Hungary and co-financed by the European Regional Development Fund. Discussions with Dr. Allan H. Harvey (NIST) and Dr. Shanshan Yu (JPL) on the topic and the data of this paper are gratefully acknowledged.

9. References

- ¹W. Lochte-Holtgreven and G. H. Dieke, *Ann. Phys.* **395**, 937 (1929).
- ²J. Curry and G. Herzberg, *Ann. Phys.* **411**, 800 (1934).
- ³H. P. Knauss and S. S. Ballard, *Phys. Rev.* **48**, 796 (1935).
- ⁴L. Herzberg and G. Herzberg, *Astrophys. J.* **105**, 353 (1947).
- ⁵H. D. Babcock and L. Herzberg, *Astrophys. J.* **108**, 167 (1948).
- ⁶J. H. Burkhalter, R. S. Anderson, W. V. Smith, and W. Gordy, *Phys. Rev.* **79**, 651 (1950).
- ⁷M. W. Feast, *Proc. Phys. Soc., Sect. A* **63**, 549 (1950).
- ⁸R. S. Anderson, C. M. Johnson, and W. Gordy, *Phys. Rev.* **83**, 1061 (1951).
- ⁹B. V. Gokhale and M. W. P. Strandberg, *Phys. Rev.* **84**, 844 (1951).
- ¹⁰G. Herzberg, *Can. J. Phys.* **30**, 185 (1952).
- ¹¹G. Herzberg, *Can. J. Phys.* **31**, 657 (1953).
- ¹²P. Brix and G. Herzberg, *Can. J. Phys.* **32**, 110 (1954).
- ¹³M. Mizushima and R. M. Hill, *Phys. Rev.* **93**, 745 (1954).
- ¹⁴R. W. Zimmerer and M. Mizushima, *Phys. Rev.* **121**, 152 (1961).
- ¹⁵L. Wallace, *Astrophys. J. Suppl. Ser.* **7**, 165 (1962).
- ¹⁶B. G. West and M. Mizushima, *Phys. Rev.* **143**, 31 (1966).
- ¹⁷F. Alberti, R. A. Ashby, and A. E. Douglas, *Can. J. Phys.* **46**, 337 (1968).
- ¹⁸J. S. McKnight and W. Gordy, *Phys. Rev. Lett.* **21**, 1787 (1968).
- ¹⁹V. Degen, *Can. J. Phys.* **46**, 783 (1968).
- ²⁰D. E. Burch and D. A. Gryvnak, *Appl. Opt.* **8**, 1493 (1969).
- ²¹M. Ackerman and F. Biaume, *J. Mol. Spectrosc.* **35**, 73 (1970).
- ²²P. H. Krupenie, *J. Phys. Chem. Ref. Data* **1**, 423 (1972).
- ²³T. Amano and E. Hirota, *J. Mol. Spectrosc.* **53**, 346 (1974).
- ²⁴W. H. Fletcher and J. S. Rayside, *J. Raman Spectrosc.* **2**, 3 (1974).
- ²⁵J. W. C. Johns and D. W. Lepard, *J. Mol. Spectrosc.* **55**, 374 (1975).
- ²⁶L. Tomuta, M. Mizushima, C. J. Howard, and K. M. Evenson, *Phys. Rev. A* **12**, 974 (1975).
- ²⁷M. Ogawa, K. Yamawaki, A. Hashizume, and Y. Tanaka, *J. Mol. Spectrosc.* **55**, 425 (1975).
- ²⁸H. Liebe, G. Grimmetstad, and J. Hopponen, *IEEE Trans. Antennas Propag.* **25**, 327 (1977).
- ²⁹M. Loëte and H. Berger, *J. Mol. Spectrosc.* **68**, 317 (1977).
- ³⁰D. H. Katayama, S. Ogawa, M. Ogawa, and Y. Tanaka, *J. Chem. Phys.* **67**, 2132 (1977).
- ³¹J. W. Brault, *J. Mol. Spectrosc.* **80**, 384 (1980).
- ³²C. Amiot and J. Verges, *Can. J. Phys.* **59**, 1391 (1981).
- ³³H. G. M. Edwards, D. A. Long, K. A. B. Najm, and M. Thomsen, *J. Raman Spectrosc.* **10**, 60 (1981).
- ³⁴A. Scalabrin, R. J. Saykally, K. M. Evenson, H. Radford, and M. Mizushima, *J. Mol. Spectrosc.* **89**, 344 (1981).
- ³⁵Y. Endo and M. Mizushima, *Jpn. J. Appl. Phys., Part 2* **21**, L379 (1982).
- ³⁶G. Cazzoli, C. Esposti, and P. Favero, *Chem. Phys. Lett.* **100**, 99 (1983).
- ³⁷K. Yoshino, D. E. Freeman, and W. H. Parkinson, *J. Phys. Chem. Ref. Data* **13**, 207 (1984).

- ³⁸K. W. Hillig, C. C. Chiu, W. G. Read, and E. Cohen, *J. Mol. Spectrosc.* **109**, 205 (1985).
- ³⁹C. M. L. Kerr and J. K. G. Watson, *Can. J. Phys.* **64**, 36 (1986).
- ⁴⁰P. M. Borrell, P. Borrell, and D. A. Ramsay, *Can. J. Phys.* **64**, 721 (1986).
- ⁴¹B. Coquart and D. A. Ramsay, *Can. J. Phys.* **64**, 726 (1986).
- ⁴²E. H. Fink, H. Kruse, D. A. Ramsay, and M. Vervloet, *Can. J. Phys.* **64**, 242 (1986).
- ⁴³D. A. Ramsay, *Can. J. Phys.* **64**, 717 (1986).
- ⁴⁴J. C. Nieh and J. J. Valentini, *J. Phys. Chem.* **91**, 1370 (1987).
- ⁴⁵L. Zink and M. Mizushima, *J. Mol. Spectrosc.* **125**, 154 (1987).
- ⁴⁶T. G. Slanger and P. C. Cosby, *J. Phys. Chem.* **92**, 267 (1988).
- ⁴⁷H. Kanamori, M. Momona, and K. Sakurai, *Can. J. Phys.* **68**, 313 (1990).
- ⁴⁸A. Sur, R. S. Friedman, and P. J. Miller, *J. Chem. Phys.* **94**, 1705 (1991).
- ⁴⁹K. W. Brown, N. H. Rich, and J. W. Nibler, *J. Mol. Spectrosc.* **151**, 482 (1992).
- ⁵⁰G. Rouillé, G. Millot, R. Saint-Loup, and H. Berger, *J. Mol. Spectrosc.* **154**, 372 (1992).
- ⁵¹S. Katsumata and K. Kimura, *Appl. Spectrosc. Rev.* **27**, 193 (1992).
- ⁵²C. Chen and D. Ramsay, *J. Mol. Spectrosc.* **160**, 512 (1993).
- ⁵³K. Yoshino, J. E. Murray, J. R. Esmond, Y. Sun, W. H. Parkinson, A. P. Thorne, R. C. M. Learner, and G. Cox, *Can. J. Phys.* **72**, 1101 (1994).
- ⁵⁴B. R. Lewis, J. P. England, R. J. Winkel, S. S. Banerjee, P. M. Dooley, S. T. Gibson, and K. G. H. Baldwin, *Phys. Rev. A* **52**, 2717 (1995).
- ⁵⁵E. Cohen, M. Okunishi, and J. Oh, *J. Mol. Struct.* **352-353**, 283 (1995).
- ⁵⁶A.-C. Cheung, K. Yoshino, J. Esmond, and W. Parkinson, *J. Mol. Spectrosc.* **178**, 66 (1996).
- ⁵⁷G. Millot, B. Lavorel, and G. Fanjoux, *J. Mol. Spectrosc.* **176**, 211 (1996).
- ⁵⁸K. Park, I. Nolt, T. Steele, L. Zink, K. Evenson, K. Chance, and A. Murray, *J. Quant. Spectrosc. Radiat. Transfer* **56**, 315 (1996).
- ⁵⁹J. P. England, B. R. Lewis, S. T. Gibson, and M. L. Ginter, *J. Chem. Phys.* **104**, 2765 (1996).
- ⁶⁰L. Biennier and A. Campargue, *J. Mol. Spectrosc.* **188**, 248 (1998).
- ⁶¹L. Gianfrani, R. W. Fox, and L. Hollberg, *J. Opt. Soc. Am. B* **16**, 2247 (1999).
- ⁶²H. Naus, K. Navaian, and W. Ubachs, *Spectrochim. Acta Part A: Mol. Biomol. Spectrosc.* **55**, 1255 (1999).
- ⁶³H. Naus and W. Ubachs, *J. Mol. Spectrosc.* **193**, 442 (1999).
- ⁶⁴K. Yoshino, J. R. Esmond, W. H. Parkinson, A. P. Thorne, R. C. M. Learner, and G. Cox, *J. Chem. Phys.* **111**, 2960 (1999).
- ⁶⁵L. Brown and C. Plymate, *J. Mol. Spectrosc.* **199**, 166 (2000).
- ⁶⁶S.-L. Cheah, Y.-P. Lee, and J. Ogilvie, *J. Quant. Spectrosc. Radiat. Transfer* **64**, 467 (2000).
- ⁶⁷K. Yoshino, J. R. Esmond, W. H. Parkinson, A. P. Thorne, R. C. M. Learner, G. Cox, and A. S.-C. Cheung, *J. Chem. Phys.* **112**, 9791 (2000).
- ⁶⁸L. C. O'Brien, H. Cao, and J. J. O'Brien, *J. Mol. Spectrosc.* **207**, 99 (2001).
- ⁶⁹M.-F. Mérienne, A. Jenouvier, B. Coquart, M. Carleer, S. Fally, R. Colin, A. Vandaele, and C. Hermans, *J. Mol. Spectrosc.* **207**, 120 (2001).
- ⁷⁰A. Krupnov, G. Golubiatnikov, V. Markov, and D. Sergeev, *J. Mol. Spectrosc.* **215**, 309 (2002).
- ⁷¹S. Brodersen and J. Bendtsen, *J. Mol. Spectrosc.* **219**, 248 (2003).
- ⁷²G. Golubiatnikov and A. Krupnov, *J. Mol. Spectrosc.* **217**, 282 (2003).
- ⁷³T. Matsui, A.-C. Cheung, K.-S. Leung, K. Yoshino, W. Parkinson, A. Thorne, J. Murray, K. Ito, and T. Imajo, *J. Mol. Spectrosc.* **219**, 45 (2003).
- ⁷⁴M. Gupta, T. Owano, D. S. Baer, A. O'Keefe, and S. Williams, *Chem. Phys. Lett.* **400**, 42 (2004).
- ⁷⁵N. J. van Leeuwen, H. G. Kjaergaard, D. L. Howard, and A. C. Wilson, *J. Mol. Spectrosc.* **228**, 83 (2004).
- ⁷⁶M. Tretyakov, G. Golubiatnikov, V. Parshin, M. Koshelev, S. Myasnikova, A. Krupnov, and P. Rosenkranz, *J. Mol. Spectrosc.* **223**, 31 (2004).
- ⁷⁷S. Williams, M. Gupta, T. Owano, D. S. Baer, A. O'Keefe, D. R. Yarkony, and S. Matsika, *Opt. Lett.* **29**, 1066 (2004).
- ⁷⁸S. Hannemann, E.-J. van Duijn, and W. Ubachs, *J. Mol. Spectrosc.* **232**, 151 (2005).
- ⁷⁹M. Tretyakov, M. Koshelev, V. Dorovskikh, D. Makarov, and P. Rosenkranz, *J. Mol. Spectrosc.* **231**, 1 (2005).
- ⁸⁰D. J. Robichaud, J. T. Hodges, P. Masłowski, L. Y. Yeung, M. Okumura, C. E. Miller, and L. R. Brown, *J. Mol. Spectrosc.* **251**, 27 (2008).
- ⁸¹A. Predoi-Cross, K. Hambrook, R. Keller, C. Povey, I. Schofield, D. Hurtmans, H. Over, and G. C. Mellau, *J. Mol. Spectrosc.* **248**, 85 (2008).
- ⁸²T. Földes, P. Čermák, M. Macko, P. Veis, and P. Macko, *Chem. Phys. Lett.* **467**, 233 (2009).
- ⁸³B. J. Drouin, S. Yu, C. E. Miller, H. S. Müller, F. Lewen, S. Brünken, and H. Habara, *J. Quant. Spectrosc. Radiat. Transfer* **111**, 1167 (2010).
- ⁸⁴I. E. Gordon, S. Kassi, A. Campargue, and G. C. Toon, *J. Quant. Spectrosc. Radiat. Transfer* **111**, 1174 (2010).
- ⁸⁵O. Leshchishina, S. Kassi, I. E. Gordon, L. S. Rothman, L. Wang, and A. Campargue, *J. Quant. Spectrosc. Radiat. Transfer* **111**, 2236 (2010).
- ⁸⁶I. E. Gordon, L. S. Rothman, and G. C. Toon, *J. Quant. Spectrosc. Radiat. Transfer* **112**, 2310 (2011).
- ⁸⁷T. G. Slanger, unpublished data cited in Ref. 94 (2011).
- ⁸⁸J. Domyslawska, S. Wójciewicz, D. Lisak, A. Cygan, F. Ozimek, K. Stec, C. Radzewicz, R. S. Trawiński, and R. Ciuryło, *J. Chem. Phys.* **136**, 024201 (2012).
- ⁸⁹B. J. Drouin, H. Gupta, S. Yu, C. E. Miller, and H. S. P. Müller, *J. Chem. Phys.* **137**, 024305 (2012).
- ⁹⁰C. E. Miller and D. Wunch, *J. Quant. Spectrosc. Radiat. Transfer* **113**, 1043 (2012).
- ⁹¹J. J. O'Brien, E. C. O'Brien, and L. C. O'Brien, *J. Mol. Spectrosc.* **273**, 34 (2012).
- ⁹²S. Yu, C. E. Miller, B. J. Drouin, and H. S. P. Müller, *J. Chem. Phys.* **137**, 024304 (2012).
- ⁹³B. J. Drouin, S. Yu, B. M. Elliott, T. J. Crawford, and C. E. Miller, *J. Chem. Phys.* **139**, 144301 (2013).
- ⁹⁴S. Yu, B. J. Drouin, and C. E. Miller, *J. Chem. Phys.* **141**, 174302 (2014).
- ⁹⁵S. Wójciewicz, A. Cygan, P. Masłowski, J. Domyslawska, D. Lisak, R. Trawiński, and R. Ciuryło, *J. Quant. Spectrosc. Radiat. Transfer* **144**, 36 (2014).
- ⁹⁶J. Domyslawska, S. Wójciewicz, P. Masłowski, A. Cygan, K. Bielska, R. S. Trawiński, R. Ciuryło, and D. Lisak, *J. Quant. Spectrosc. Radiat. Transfer* **155**, 22 (2015).
- ⁹⁷J. Domyslawska, S. Wójciewicz, P. Masłowski, A. Cygan, K. Bielska, R. S. Trawiński, R. Ciuryło, and D. Lisak, *J. Quant. Spectrosc. Radiat. Transfer* **169**, 111 (2016).
- ⁹⁸K. Bielska, S. Wójciewicz, P. Morzyński, P. Ablewski, A. Cygan, M. Bober, J. Domyslawska, M. Zawada, R. Ciuryło, P. Masłowski, and D. Lisak, *J. Quant. Spectrosc. Radiat. Transfer* **201**, 156 (2017).
- ⁹⁹B. J. Drouin, D. C. Benner, L. R. Brown, M. J. Cich, T. J. Crawford, V. M. Devi, A. Guillaume, J. T. Hodges, E. J. Mlawer, D. J. Robichaud, F. Oyafuso, V. H. Payne, K. Sung, E. H. Wishnow, and S. Yu, *J. Quant. Spectrosc. Radiat. Transfer* **186**, 118 (2017).
- ¹⁰⁰K. Huber and G. Herzberg, *Molecular Spectra and Molecular Structure. IV. Constants of Diatomic Molecule* (Van Nostrand Reinhold Company, New York, 1979).
- ¹⁰¹H. H. Michels, in *Advances in Chemical Physics*, Vol. 45 (John Wiley & Sons, New York, 2007), pp. 225–340.
- ¹⁰²J. T. Vanderslice, E. A. Mason, and W. G. Maisch, *J. Chem. Phys.* **32**, 515 (1960).
- ¹⁰³H. F. Schaefer and F. E. Harris, *J. Chem. Phys.* **48**, 4946 (1968).
- ¹⁰⁴N. H. F. Beebe, E. W. Thulstrup, and A. Andersen, *J. Chem. Phys.* **64**, 2080 (1976).
- ¹⁰⁵R. P. Saxon and B. Liu, *J. Chem. Phys.* **67**, 5432 (1977).
- ¹⁰⁶H. Liu, D. Shi, J. Sun, Z. Zhu, and Z. Shulin, *Spectrochim. Acta Part A: Mol. Biomol. Spectrosc.* **124**, 216 (2014).
- ¹⁰⁷I. Gordon, L. Rothman, C. Hill, R. Kochanov, Y. Tan, P. Bernath, M. Birk, V. Boudon, A. Campargue, K. Chance, B. Drouin, J.-M. Flaud, R. Gamache, J. Hodges, D. Jacquemart, V. Perevalov, A. Perrin, K. Shine, M.-A. Smith, J. Tennyson, G. Toon, H. Tran, V. Tyuterev, A. Barbe, A. Császár, V. Devi, T. Furtenbacher, J. Harrison, J.-M. Hartmann, A. Jolly, T. Johnson, T. Karman, I. Kleiner, A. Kyuberis, J. Loos, O. Lyulin, S. Massie, S. Mikhailenko, N. Moazzen-Ahmadi, H. Müller, O. Naumenko, A. Nikitin, O. Polyansky, M. Rey, M. Rotger, S. Sharpe, K. Sung, E. Starikova, S. Tashkun, J. V. Auwera, G. Wagner, J. Wilzewski, P. Wcislo, S. Yu, and E. Zak, *J. Quant. Spectrosc. Radiat. Transfer* **203**, 3 (2017).

- ¹⁰⁸T. Furtenbacher, A. G. Császár, and J. Tennyson, *J. Mol. Spectrosc.* **245**, 115 (2007).
- ¹⁰⁹T. Furtenbacher and A. G. Császár, *J. Quant. Spectrosc. Radiat. Transfer* **113**, 929 (2012).
- ¹¹⁰A. G. Császár, T. Furtenbacher, and P. Árendás, *J. Phys. Chem. A* **120**, 8949 (2016).
- ¹¹¹R. Tóbiás, T. Furtenbacher, and A. G. Császár, *J. Quant. Spectrosc. Radiat. Transfer* **203**, 557 (2017).
- ¹¹²R. Tóbiás, T. Furtenbacher, J. Tennyson, and A. G. Császár, *Phys. Chem. Chem. Phys.* **21**, 3473 (2019).
- ¹¹³A. G. Császár and T. Furtenbacher, *J. Mol. Spectrosc.* **266**, 99 (2011).
- ¹¹⁴T. Furtenbacher and A. G. Császár, *J. Mol. Struct.* **1009**, 123 (2012).
- ¹¹⁵T. Furtenbacher, I. Szabó, A. G. Császár, P. F. Bernath, S. N. Yurchenko, and J. Tennyson, *Astrophys. J. Suppl. Ser.* **224**, 44 (2016).
- ¹¹⁶L. K. McKemmish, T. Masseron, S. Sheppard, E. Sandeman, Z. Schofield, T. Furtenbacher, A. G. Császár, J. Tennyson, and C. Sousa-Silva, *Astrophys. J. Suppl. Ser.* **228**, 15 (2017).
- ¹¹⁷L. K. McKemmish, J. Borsovszky, K. L. Goodhew, S. Sheppard, A. F. V. Bennett, A. D. J. Martin, A. Singh, C. A. J. Sturgeon, T. Furtenbacher, A. G. Császár, and J. Tennyson, *Astrophys. J.* **867**, 33 (2018).
- ¹¹⁸T. Furtenbacher, T. Szidarovszky, C. Fábri, and A. G. Császár, *Phys. Chem. Chem. Phys.* **15**, 10181 (2013).
- ¹¹⁹T. Furtenbacher, T. Szidarovszky, E. Mátyus, C. Fábri, and A. G. Császár, *J. Chem. Theory Comput.* **9**, 5471 (2013).
- ¹²⁰J. Tennyson, P. F. Bernath, L. R. Brown, A. Campargue, M. R. Carleer, A. G. Császár, R. R. Gamache, J. T. Hodges, A. Jenouvier, O. V. Naumenko, O. L. Polyansky, L. S. Rothman, R. A. Toth, A. C. Vandaele, N. F. Zobov, L. Daumont, A. Z. Fazliev, T. Furtenbacher, I. E. Gordon, S. N. Mikhailyenko, and S. V. Shirin, *J. Quant. Spectrosc. Radiat. Transfer* **110**, 573 (2009).
- ¹²¹J. Tennyson, P. F. Bernath, L. R. Brown, A. Campargue, A. G. Császár, L. Daumont, R. R. Gamache, J. T. Hodges, O. V. Naumenko, O. L. Polyansky, L. S. Rothman, R. A. Toth, A. C. Vandaele, N. F. Zobov, S. Fally, A. Z. Fazliev, T. Furtenbacher, I. E. Gordon, S.-M. Hu, S. N. Mikhailyenko, and B. A. Voronin, *J. Quant. Spectrosc. Radiat. Transfer* **111**, 2160 (2010).
- ¹²²J. Tennyson, P. F. Bernath, L. R. Brown, A. Campargue, A. G. Császár, L. Daumont, R. R. Gamache, J. T. Hodges, O. V. Naumenko, O. L. Polyansky, L. S. Rothman, A. C. Vandaele, N. F. Zobov, A. R. Al Derzi, C. Fábri, A. Z. Fazliev, T. Furtenbacher, I. E. Gordon, L. Lodi, and I. I. Mizus, *J. Quant. Spectrosc. Radiat. Transfer* **117**, 29 (2013).
- ¹²³J. Tennyson, P. F. Bernath, L. R. Brown, A. Campargue, A. G. Császár, L. Daumont, R. R. Gamache, J. T. Hodges, O. V. Naumenko, O. L. Polyansky, L. S. Rothman, A. C. Vandaele, N. F. Zobov, N. Dénes, A. Z. Fazliev, T. Furtenbacher, I. E. Gordon, S.-M. Hu, T. Szidarovszky, and I. A. Vasilenko, *J. Quant. Spectrosc. Radiat. Transfer* **142**, 93 (2014).
- ¹²⁴J. Tennyson, P. F. Bernath, L. R. Brown, A. Campargue, A. G. Császár, L. Daumont, R. R. Gamache, J. T. Hodges, O. V. Naumenko, O. L. Polyansky, L. S. Rothman, A. C. Vandaele, and N. F. Zobov, *Pure Appl. Chem.* **86**, 71 (2014).
- ¹²⁵K. L. Chubb, O. Naumenko, S. Kelly, S. Bartoletto, S. Macdonald, M. Mukhtar, A. Grachov, J. White, E. Coleman, A. Liu, A. Z. Fazliev, E. R. Polovtseva, V.-M. Horneman, A. Campargue, T. Furtenbacher, A. G. Császár, S. N. Yurchenko, and J. Tennyson, *J. Quant. Spectrosc. Radiat. Transfer* **218**, 178 (2018).
- ¹²⁶R. Tóbiás, T. Furtenbacher, A. G. Császár, O. V. Naumenko, J. Tennyson, J.-M. Flaud, P. Kumar, and B. Poirier, *J. Quant. Spectrosc. Radiat. Transfer* **208**, 152 (2018).
- ¹²⁷K. L. Chubb, M. Joseph, J. Franklin, N. Choudhury, T. Furtenbacher, A. G. Császár, G. Gaspard, P. Oguoko, A. Kelly, S. N. Yurchenko, J. Tennyson, and C. Sousa-Silva, *J. Quant. Spectrosc. Radiat. Transfer* **204**, 42 (2018).
- ¹²⁸A. R. Al Derzi, T. Furtenbacher, J. Tennyson, S. N. Yurchenko, and A. G. Császár, *J. Quant. Spectrosc. Radiat. Transfer* **161**, 117 (2015).
- ¹²⁹C. Fábri, E. Mátyus, T. Furtenbacher, L. Nemes, B. Mihály, T. Zoltáni, and A. G. Császár, *J. Chem. Phys.* **135**, 094307 (2011).
- ¹³⁰T. Furtenbacher, T. Szidarovszky, J. Hrubý, A. A. Kyuberis, N. F. Zobov, O. L. Polyansky, J. Tennyson, and A. G. Császár, *J. Phys. Chem. Ref. Data* **45**, 043104 (2016).
- ¹³¹I. Simkó, T. Furtenbacher, J. Hrubý, N. F. Zobov, O. L. Polyansky, J. Tennyson, R. R. Gamache, T. Szidarovszky, N. Dénes, and A. G. Császár, *J. Phys. Chem. Ref. Data* **46**, 023104 (2017).
- ¹³²D. A. McQuarrie, *Statistical Mechanics* (University Science Books, Sausalito, 2000).
- ¹³³R. Schmidt and W. Wagner, *Fluid Phase Equilib.* **19**, 175 (1985).
- ¹³⁴W. Wagner, J. Ewers, and R. Schmidt, *Ber. Bunsenges. Phys. Chem.* **86**, 538 (1982).
- ¹³⁵H. P. Broida and A. G. Gaydon, *Proc. R. Soc. A* **222**, 181 (1954).
- ¹³⁶J. L. Richards and P. M. Johnson, *J. Chem. Phys.* **65**, 3948 (1976).
- ¹³⁷L. Herman, R. Herman, and D. Rakotoarijimy, *J. Phys. Radium* **22**, 1 (1961).
- ¹³⁸V. Degen and R. W. Nicholls, *J. Geophys. Res.* **71**, 3781 (1966).
- ¹³⁹C. A. Barth and J. Kaplan, *J. Mol. Spectrosc.* **3**, 583 (1959).
- ¹⁴⁰C. A. Barth and M. Patapoff, *Astrophys. J.* **136**, 1144 (1962).
- ¹⁴¹T. G. Slanger, P. C. Cosby, D. L. Huestis, and A. M. Widhalm, *Ann. Geophys.* **22**, 3305 (2004).
- ¹⁴²P. C. Cosby, B. D. Sharpee, T. G. Slanger, D. L. Huestis, and R. W. Hanuschik, *J. Geophys. Res.* **111**, A12, <https://doi.org/10.1029/2006ja012023> (2006).
- ¹⁴³S. Yang, M. R. Canagaratna, S. K. Witonsky, S. L. Coy, J. I. Steinfield, R. Field, and A. A. Kachanov, *J. Mol. Spectrosc.* **201**, 188 (2000).
- ¹⁴⁴R. Schermaul and R. C. M. Learner, *J. Quant. Spectrosc. Radiat. Transfer* **61**, 781 (1999).
- ¹⁴⁵D. J. Robichaud, "High-resolution study of the O₂ A-band using frequency stabilized cavity ring-down spectroscopy," Ph.D. dissertation, California Institute of Technology, Pasadena, California, 2008.
- ¹⁴⁶G. H. Dieke and H. D. Babcock, *Proc. Natl. Acad. Sci. U. S. A.* **13**, 670 (1927).
- ¹⁴⁷A. Jenouvier, M.-F. Mérienne, B. Coquart, M. Carleer, S. Fally, A. C. Vandaele, C. Hermans, and R. Colin, *J. Mol. Spectrosc.* **198**, 136 (1999).
- ¹⁴⁸W. H. Hocking, M. C. L. Gerry, and A. J. Merer, *Can. J. Phys.* **57**, 54 (1979).
- ¹⁴⁹J. Brown, A.-C. Cheung, and A. Merer, *J. Mol. Spectrosc.* **124**, 464 (1987).
- ¹⁵⁰A.-C. Cheung, K. Yoshino, W. Parkinson, and D. Freeman, *J. Mol. Spectrosc.* **119**, 1 (1986).
- ¹⁵¹*Thermodynamic Properties of Individual Substances. Volume 1, Part Two: Tables*, edited by L. V. Gurvich, I. V. Veyts, and C. B. Alcock (Hemisphere Publishing Corporation, New York, 1989).
- ¹⁵²M. Capitelli, G. Colonna, D. Giordano, L. Marrappa, A. Casavola, P. Minelli, D. Pagano, L. D. Pietanza, F. Taccogna, and B. Warmbein, "Tables of internal partition functions and thermodynamic properties of high-temperature mars-atmosphere species from 50 K to 50000 K," Technical Report No. STR-246, ESA Scientific Technical Review, 2005.
- ¹⁵³H. W. Woolley, *J. Res. Natl. Bur. Stand.* **40**, 163 (1948).
- ¹⁵⁴R. R. Gamache, C. Roller, E. Lopes, I. E. Gordon, L. S. Rothman, O. L. Polyansky, N. F. Zobov, A. A. Kyuberis, J. Tennyson, S. N. Yurchenko, A. G. Császár, T. Furtenbacher, X. Huang, D. W. Schwenke, T. J. Lee, B. J. Drouin, S. A. Tashkin, V. I. Perevalov, and R. V. Kochanov, *J. Quant. Spectrosc. Radiat. Transfer* **203**, 70 (2017).
- ¹⁵⁵P. S. Barklem and R. Collet, *Astron. Astrophys.* **588**, A96 (2016).
- ¹⁵⁶S. C. F. Rossi, W. J. Maciel, and P. Benevides-Soares, *Astron. Astrophys.* **148**, 93 (1985).
- ¹⁵⁷A. W. Irwin, *Astrophys. J. Suppl. Ser.* **45**, 621 (1981).
- ¹⁵⁸B. McBride, *Thermodynamic Properties to 6000 Degrees K for 210 Substances Involving the First 18 Elements*, National Aeronautics and Space Administration special paper (Office of Scientific and Technical Information, National Aeronautics and Space Administration, Washington, DC, 1963).
- ¹⁵⁹See <http://janaf.nist.gov> for JANAF thermochemical tables, NIST standard reference database 13 (1998).
- ¹⁶⁰R. T. Jacobsen, R. B. Stewart, and A. F. Myers, in *Advances in Cryogenic Engineering*, Vol. 18 (Springer, US, 1973), pp. 248–255.